J|A|C|S ARTICLES

Published on Web 03/24/2009

A Solid-State NMR Study of Lead and Vanadium Substitution into Hydroxyapatite

Hélène Pizzala,[‡] Stefano Caldarelli,*[,†] Jean-Guillaume Eon,[§] Alexandre Malta Rossi,[⊥] Danielle Laurencin,[¶] and Mark E. Smith[¶]

Aix Marseille Université, ISm2 UMR 6263, Campus de Saint Jérôme, Service 511 F-13013 Marseille France, Universités Aix-Marseille I, II et III − CNRS, UMR 6264 Laboratoire Chimie Provence, Spectrométries Appliquées à la Chimie Structurale, F-13397 Marseille, France, Instituto de Quumica, Universidade Federal do Rio de Janeiro, Rio de Janeiro, Brazil, Centro Brasileiro de Pesquisas Fısicas, Rio de Janeiro, Brazil, Department of Physics, University of Warwick, Coventry, U.K. CV4 7AL

Received October 21, 2008; E-mail: s.caldarelli@univ-cezanne.fr

Abstract: A systematic study on cationic and anionic substitution in hydroxyapatite structures was carried out, with the aim of understanding the impact of ion exchange on the crystalline structure and properties of these materials. Lead and vanadium were chosen for the exchange, due to their known effects on the redox and catalytic properties of hydroxypatites. Hydroxyapatites with variable Pb and V contents, Pb_x-$Ca_{10-x}(VO_4)_y(PO_4)_{6-y}(OH)_2$ ($x = 0$, 2, 4, 6, 8 and 10 for $y = 1$; $y = 0$, 0.5, 1, 2, 3 and 6 for $x = 10$) were synthesized and characterized by NMR spectroscopy. Solid-state NMR allowed an analysis of the chemical environment of every ion after substitution into the hydroxyapatite network. ^{43}Ca and ^{207}Pb NMR spectra at different lead concentrations provided clear evidence of the preferential substitution of lead into the Ca(II) site, the replacement of the Ca(I) site starting at $x = 4$ for $y = 1$. Two NMR distinguishable Pb(I) sites were observed in $Pb_{10}(PO_4)_6(OH)_2$, which is compatible with the absence of a local mirror plane perpendicular to the *c* direction. In contrast with ^{31}P NMR, for which only small variations related to the incorporation of Pb are observed, the strong change in the ^{51}V NMR spectrum indicates that lead perturbs the vanadium environment more than the phosphorus one. The existence of a wide variety of environments for OH in substituted apatites is revealed by ^{1}H NMR, and the mobility of the water molecules appears to vary upon introduction of lead into the structure.

Introduction

The description of cationic and anionic exchange into apatite structures attracts considerable interest due to the large range of applications of these materials. In fact, apatites are the most common natural source of phosphates[1] and, among other possible applications, have been shown to be able to capture and store a large variety of metals from the environment,[2−4] or to act as catalysts.[5,6] Additionally, hydroxyapatites (HA) are natural constituents of bones and teeth, and thus one of the most commonly used bioceramics for bone regeneration.[7]

The uptake of heavy metals by hydroxyapatites has been under investigation for several years, mainly from the perspective of environmental applications, because of the ability of this material to immobilize heavy metals over a large range of pH.[8] Lead is one of the most studied metals because of its high toxicity. It has been shown that powdered samples of lead−calcium apatite, $Pb_xCa_{10-x}(PO_4)_6(OH)_2$, can be prepared over the whole composition range, i.e. $0 \le x \le 10$. In the most common hexagonal hydroxyapatite structure of space group $P6_3/m$, $Ca(I)_4Ca(II)_6(PO_4)_6(OH)_2$, the 9-fold 4f and 7-fold 6h sites Ca(I) and Ca(II) are both available for cationic substitution. The first analyses of the variation of the lattice parameters and frequency of the OH infrared band indicated a heterogeneous distribution of Pb between these two cationic sites.[9] Subsequently, Raman and FTIR spectroscopies were used to follow the structural evolution in hydroxyapatite related to the progressive substitution of Pb for Ca,[10] and the splitting of the ν(OH) band suggested the preference of lead for the Ca(II) site. The evolution

† Aix Marseille Université, ISm2 UMR 6263.
‡ Universités Aix-Marseille I, II et III − CNRS, UMR 6264.
§ Universidade Federal do Rio de Janeiro.
⊥ Centro Brasileiro de Pesquisas Fısicas.
¶ University of Warwick.

(1) White, T.; Ferraris, C.; Kim, J.; Madhavi, S. In *Micro- and Mesoporous Mineral Phases*; Ferraris, G., Merlino, S., Eds.; Mineralogical Society of America: Washington, DC, 2005; Vol. 57, p 307−401.
(2) Ma, Q. Y.; Logan, T. J.; Traina, S. J. *Environ. Sci. Technol.* **1995**, *29*, 1118–1126.
(3) Ruby, M. V.; Davis, A.; Nicholson, A. *Environ. Sci. Technol.* **1994**, *28*, 646–654.
(4) Xu, Y. P.; Schwartz, F. W. *J. Contam. Hydrol.* **1994**, *15*, 187–206.
(5) Boechat, C. B.; Terra, J.; Eon, J. G.; Ellis, D. E.; Rossi, A. M. *Phys. Chem. Chem. Phys.* **2003**, *5*, 4290–4298.
(6) Ikram, M.; Ahmed, H.; Mendes, P.; Mir, F. A.; Bashir, A.; Paula, A.; Rossi, A. M.; Eon, J. G. *Mod. Phys. Lett., B* **2007**, *21*, 1489–1500.
(7) Elliott, J. C. *Structure and Chemistry of the Apatites and Other Calcium Orthophosphates*; Elsevier: Amsterdam, New York, 1994; Vol. 18.
(8) Zhang, P. C.; Ryan, J. A.; Yang, J. *Environ. Sci. Technol.* **1998**, *32*, 2763–2768.
(9) Bigi, A.; Gandolfi, M.; Gazzano, M.; Ripamonti, A.; Roveri, N.; Thomas, S. A. *J. Chem. Soc., Dalton Trans.* **1991**, 2883–2886.
(10) Hadrich, A.; Lautié, A.; Mhiri, T. *Spectrochim. Acta, Part A* **2001**, *A57*, 1673–1681.

of the intensity and position of the hydroxyl and phosphate bands was interpreted by the progressive formation of partly covalent Pb−O bonds and by changes in hydrogen bonding involving the hydroxyls. However, further evidence of the presence of hydrogen bonding in natural and artificial hydroxyapatites has not yet been conclusive. More recently, solid solutions of lead−calcium apatites prepared by a hydrothermal method were studied by XRD using Rietveld refinement,[11] and reinforced the FTIR suggestions that lead has a strong preference for the Ca(II) site. Density functional theoretical analyses also led to the conclusion that energetic criteria favor Pb substitution into the Ca(II) site. XRD Rietveld refinements and simulations of the Pb L-edge EXAFS spectra of $Pb_{3.4}Ca_{6.6}(PO_4)_6(OH)_2$, however, also indicate a partial occupation of the Ca(I) site.[12]

The substitution of phosphate ions by vanadate ions in hydroxyapatites has been extensively studied, from the perspective of generating new apatite-based materials with redox properties.[5] Hydroxyvanadinite, $Pb_{10}(VO_4)_6(OH)_2$, has been characterized by XRD, EXAFS and Raman spectroscopy.[5,13] Its electronic structure was investigated by *ab initio* methods, revealing strong covalent V−O bonds, in contrast with the weaker Pb−O ones. However, no specific interaction between the Pb and V metal centers, which could have helped explain the origin of the redox differences between hydroxyvanadinite and calcium vanadate apatite, was detected. More recently, differences in the catalytic behavior in lead and/or vanadate-exchanged hydroxyapatites[14] were observed, the structural origin of which was not addressed. As a result, in order to gain better control over the properties of apatites, it appears necessary to better understand what changes are induced by ionic substitutions in HA at the molecular level.

We present here an investigation of the structure of two series of mixed lead/vanadium hydroxyapatites, one with a fixed content of vanadium and an increasing content of lead ($Pb_xCa_{10-x}(VO_4)(PO_4)_5(OH)_2$ with $x = 0$, 2, 4, 6, 8 and 10), and the other with vanadium/phosphorus substitution ($Pb_{10}(VO_4)_y(PO_4)_{6-y}(OH)_2$ with $y = 0$, 0.5, 1, 2, 3 and 6). In this paper, solid-state NMR spectroscopy is used to precisely characterize the evolution of the local environment of the anions and cations throughout these compositions, as well as that of the water molecules.

Experimental Section

Synthesis and Sample Characterization. Solid solutions of $Pb_xCa_{10-x}(VO_4)_y(PO_4)_{6-y}(OH)_2$ ($x = 0$, 2, 4, 6, 8 and 10 for $y = 1$; $y = 0$, 0.5, 1, 2, 3 and 6 for $x = 0$) were prepared by the coprecipitation method using a 0.12 M solution of $Pb(NO_3)_2 \cdot 4H_2O$, a 0.10 M solution of Na_3VO_4 and a 0.12 M solution of $(NH_4)_2HPO_4$. Reagents were added while controlling carefully the temperature, pH, stirring velocity, addition rate and aging time. The precipitate was separated by filtration, repeatedly washed with deionized water and dried at 37 °C. The elemental concentrations were determined by inductively coupled plasma optical emission spectrometry (ICP). Infrared spectroscopy (FTIR) was used to investigate vibrational modes of PO_4^{3-}, VO_4^{3-} and OH^- groups and water molecules associated to the HA structure. The degree of crystallinity of HA structures and the absence of secondary mineral phases were verified by X-ray powder diffraction using a conventional X-ray source with a flat-plate Bragg−Brentano geometry, and graphite monochromated Cu Kα radiation. The materials were studied by NMR as made, without performing any further calcination.

NMR Spectroscopy. ^{207}Pb, ^1H, ^{31}P and ^{51}V NMR experiments were performed on a Bruker DSX 400 (9.4 T) spectrometer at Larmor frequencies of 83.77, 400.13, 161.09, and 105.26 MHz, respectively. ^{207}Pb static spectra were obtained with a double resonance (HX) 5 mm static probehead using a Hahn echo sequence. The $\pi/2$ pulse was of 2.5 μs and the echo delay 20 μs. Magic angle spinning (MAS) spectra were recorded with a 2.5 mm HX probehead, spinning up to 20 kHz and using a rotation synchronized Hahn Echo, with a $\pi/2$ pulse of 2.1 μs and an echo delay of 50 μs. The spectra were accumulated with a sweep width of 416 kHz. The recycle delay was 30 s. The chemical shift scale was calibrated with the static spectrum of crystalline $Pb(NO_3)_2$, the most intense point of which was set at −3473.5 ppm with respect to $Pb(CH_3)_4$.[15] A test of the influence of the limited pulse excitation bandwidth on the lead signal was performed on the $Pb_{10}(PO_4)_6(OH)_2$ sample. The irradiation frequency chosen produced the most informative spectra with a tolerable intensity loss and line shape distortion on the high-frequency peaks.

^1H MAS NMR spectra, referenced to TMS, were recorded on a 2.5 mm HX probehead, spinning at 25 kHz, using a Carr−Purcell−Meiboom−Gill pulse sequence to minimize the large background. The $\pi/2$ pulse length was 2.0 μs, the echo delay was 40 μs and 8 transients were accumulated with a recycle delay of 90 s. ^{31}P and ^{51}V spectra were recorded on a 4 mm HX probehead. MAS spectra were obtained spinning at 10 kHz. The ^{31}P pulse length was 1.8 μs ($\pi/3$ tip angle, for optimum experimental time due to long relaxation times), 16 transients were accumulated with a recycle delay of 120 s. The ^{51}V pulse length was 1 μs ($\pi/12$ tip angle for an adequate approximation of the linear excitation regime), and 2048 transients were accumulated with a recycle delay of 1 s. The ^{31}P and ^{51}V chemical shifts were referenced with respect to a 85% solution of H_3PO_4 (set to 0 ppm) and to crystalline V_2O_5 (with the isotropic peak set to −610 ppm), respectively, used as external standards. All echo values were chosen such as not to produce significant line shape distortions.

^{43}Ca solid-state NMR spectra were recorded on a Varian Infinity Plus 800 (18.8 T) spectrometer operating at 53.78 MHz, using a Varian 4 mm probe and spinning at 4 kHz. ^{43}Ca being a spin-7/2 low-γ nucleus[16] (i.e., with a small magnetic moment) and of low natural abundance (0.14%), rotor-assisted-population-transfer (RAPT) pulses were applied prior to the excitation in order to enhance the signal sensitivity.[17,18] The RAPT[19] sequence (sets of $+X/-X$ 2.5 μs pulses with a ∼15 kHz radiofrequency field strength), which had been previously optimized on nonsubstituted hydroxyapatite $Ca_{10}(PO_4)_6(OH)_2$,[20] was applied prior to a $\pi/2$ pulse selective for the central transition. Recycle delays of 0.1 s were used, as for $Ca_{10}(PO_4)_6(OH)_2$,[20] for which it had been shown that there was no significant change in spectral line shape with larger recycle delays. A number of transients between 1200000 and 1400000 were acquired with total experimental times of ∼48 h. All spectra were externally referenced to a 1 M aqueous solution of $CaCl_2$ at 0 ppm.

(11) Mavropoulos, E.; Rossi, A. M.; Costa, A. M.; Perez, C. A. C.; Moreira, J. C.; Aldanha, M. *Environ. Sci. Technol.* **2002**, *36*, 1625–1629.
(12) Eon, J. G.; Boechat, C. B.; Rossi, A. M.; Terra, J.; Ellis, D. E. *Phys. Chem. Chem. Phys.* **2006**, *8*, 1845–1851.
(13) Ellis, D. E.; Terra, J.; Warschkow, O.; Jiang, M.; Gonzalez, G. B.; Okasinski, J. S.; Bedzyk, J. M.; Rossi, A. M.; Eon, J.-G. *Phys. Chem. Chem. Phys.* **2006**, *8*, 967–976.
(14) Ogo, S.; Onda, A.; Yanagisawa, K. *Appl. Catal., A* **2008**, *348*, 129–134.
(15) Neue, G.; Dybowski, C.; Smith, M. L.; Hepp, M. A.; Perry, D. *Solid State NMR* **1996**, *6*, 241.
(16) MacKenzie, K. J. D.; Smith, M. E. *Multinuclear Solid-State NMR of Inorganic Materials*; Pergamon; New York, Oxford, 2002.
(17) Siegel, R.; Nakashima, T. T.; Wasylishen, R. E. *Concepts Magn. Reson. A* **2005**, *26A*, 62–77.
(18) Kwak, H. T.; Prasad, S.; Clark, T.; Grandinetti, P. J. *Solid State Nucl. Magn. Reson.* **2003**, *24*, 71–77.
(19) Madhu, P. K.; Johannessen, O. G.; Pike, K. J.; Dupree, R.; Smith, M. E.; Levitt, M. H. *J. Magn. Reson.* **2003**, *163*, 310–317.
(20) Laurencin, D.; Wong, A.; Dupree, R.; Smith, M. E. *Magn. Reson. Chem.* **2008**, *46*, 347–350.

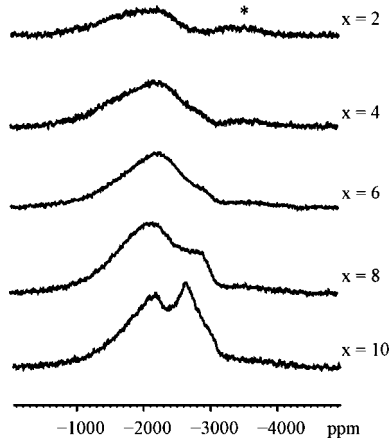

Figure 1. ^{207}Pb Hahn Echo NMR spectra of $Pb_xCa_{10-x}(VO_4)(PO_4)_5(OH)_2$ recorded at 9.4 T. The echo time was 40 μs. The environment background signal is indicated by the asterisk.

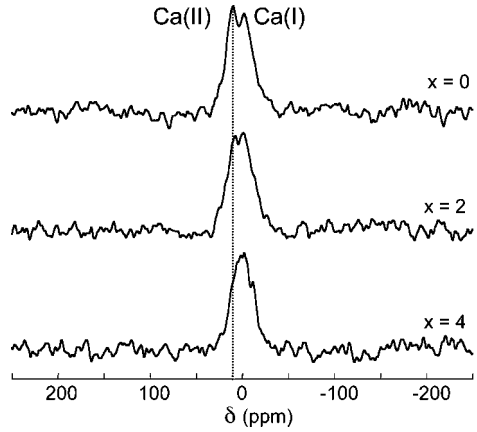

Figure 2. ^{43}Ca MAS spectra of $Pb_xCa_{10-x}(VO_4)(PO_4)_5(OH)_2$ ($x = 0$, 2, 4), recorded at 18.8 T. The MAS rate was 4 kHz.

Spectral simulations were performed with the DMFIT software.[21]

Results

1. Lead Substitution in $Pb_xCa_{10-x}(VO_4)(PO_4)_5(OH)_2$ (X Series). ^{207}Pb NMR static Hahn echo spectra of $Pb_xCa_{10-x}(VO_4)(PO_4)_5(OH)_2$ ($x = 0$, 2, 4, 6, 8 and 10) are displayed in Figure 1. Upon incorporation of lead into the structure, the progressive appearance of two broad distinct signals is observed, in agreement with the presence of two different cationic sites in the apatite structure. The overall signal intensity spreads over the chemical shift range between −800 to −3200 ppm, with maxima at −2100 and −2700 ppm. For the lower lead contents ($x < 4$), only the high-frequency signal is observed, with a line width spanning approximately 900 ppm. It is noteworthy that similar chemical shift ranges have also been observed in the ^{207}Pb NMR spectra of other lead phosphates.[22,23]

The ^{43}Ca RAPT MAS NMR spectra of the samples $Pb_xCa_{10-x}(VO_4)(PO_4)_5(OH)_2$ ($x = 0$, 2, 4) are shown in Figure 2. For $x = 0$, two distinct peaks are resolved at 11.4 and −0.6 ppm, the integrated intensity of the high-frequency signal being larger than the lower-frequency one. These peaks correspond to the Ca(II) and Ca(I) sites respectively, according to the multiple magnetic field simulations of the spectra of $Ca_{10}(PO_4)_6(OH)_2$.[20] The most striking feature as the lead content increases is the relative decrease in intensity of the high frequency component of the ^{43}Ca signal.

The influence of the lead insertion on the environment of the different anions present in the sample was also monitored. The evolution of the ^{51}V MAS NMR spectra with lead content is shown in Figure 3a. For $x = 0$, a single broad resonance is observed, with a chemical shift of −628 ppm. The corresponding static ^{51}V NMR spectrum (see Figure S1 in the Supporting Information) exhibits a signal with a small chemical shift anisotropy (less than 100 ppm), as expected for a Q^0 species.[24] For $x = 2$, the intensity of this signal decreases dramatically, while a second narrow line appears at −505 ppm. Resonances in this area are the only ones observed for higher substitution levels. As the Pb content increases, the signal becomes broader, and for $x = 10$, a shoulder is observed. The strong shift observed for most of the ^{51}V resonance between $x = 0$ and $x = 2$ indicates that the electronic environment of the anion is appreciably altered by the introduction of even a small amount of lead. However, there is no significant modification of the chemical shift anisotropy (CSA) for this resonance, indicating that the vanadate is still a Q^0 species.

The ^{31}P MAS NMR spectra of the various members of the series corresponding to progressive lead insertion are shown in Figure 3b. The ^{31}P NMR spectrum of $Ca_{10}(VO_4)(PO_4)_5(OH)_2$ exhibits a single well-resolved resonance at 2.8 ppm, as observed in $Ca_{10}(PO_4)_6(OH)_2$.[25] This resonance is shifted to −0.5 ppm for the pure lead compound $Pb_{10}(VO_4)(PO_4)_5(OH)_2$. For intermediate lead contents ($x = 2$ and 4), the phosphorus signal progressively broadens, and for higher substitution levels ($x =$ 6 and 8) an additional broad component near 1 ppm is observed. At least three lines are required to fit the latter ^{31}P spectra (see Supporting Information, Figure S2 for example), suggesting a distribution of chemical shifts induced by the incorporation of Pb.

The major features of the fast spinning rate ^{1}H MAS NMR spectra of $Ca_{10}(VO_4)(PO_4)_5(OH)_2$ are two well-resolved resonances (Figure 3c): the first at −0.2 ppm which corresponds to the hydroxyl protons and the second, broader, at about 5.0 ppm typically assigned to water molecules. In addition to these signals, two small peaks are present at ∼0.4 and ∼1.2 ppm; these are often observed on the MAS spectra of HA, but their assignment is still unclear.[26] No signal from hydrogen phosphate groups[26] is observed (the shoulder at high frequencies in the ^{1}H NMR spectrum is due to our probehead background). With increasing lead content, a shoulder clearly appears at –1.2 ppm. In the mixed phases ($x = 2$ to $x = 6$), the signal assigned to hydroxyl protons could be decomposed into at least three lines (at ∼−0.2, 0.4 and 1.2 ppm), indicating a distribution of chemical environments of the OH group. Furthermore, it is noteworthy that a significant narrowing of the H_2O and OH peaks is observed as the Pb content increases: between $x = 0$

(21) Massiot, D.; Fayon, F.; Capron, M.; King, I.; Le Calve, S.; Alonso, B.; Durand, J.; Bujoli, B.; Gan, Z.; Hoatson, G. *Magn. Reson. Chem.* **2002**, *40*, 70–76.
(22) Fechtelkord, M.; Bismayer, U. *Solid State Nucl. Magn. Reson.* **1998**, *11*, 231–241.
(23) Fayon, F.; Bessada, C.; Douy, A.; Massiot, D. *J. Magn. Reson.* **1999**, *137*, 116–121.
(24) Lapina, O. B.; Shubin, A. A.; Khabibulin, D. F.; Terskikh, V. V.; Bodart, P. R.; Amoureux, J.-P. *Catal. Today* **2003**, *78*, 91–104.
(25) Rothwell, W. P.; Waugh, J. S.; Yesinowski, J. S. *J. Am. Chem. Soc.* **1980**, *102*, 2637–2643.
(26) Jager, C.; Welzel, T.; Meyer-Zaika, W.; Epple, M. *Magn. Reson. Chem.* **2006**, *44*, 573–580.

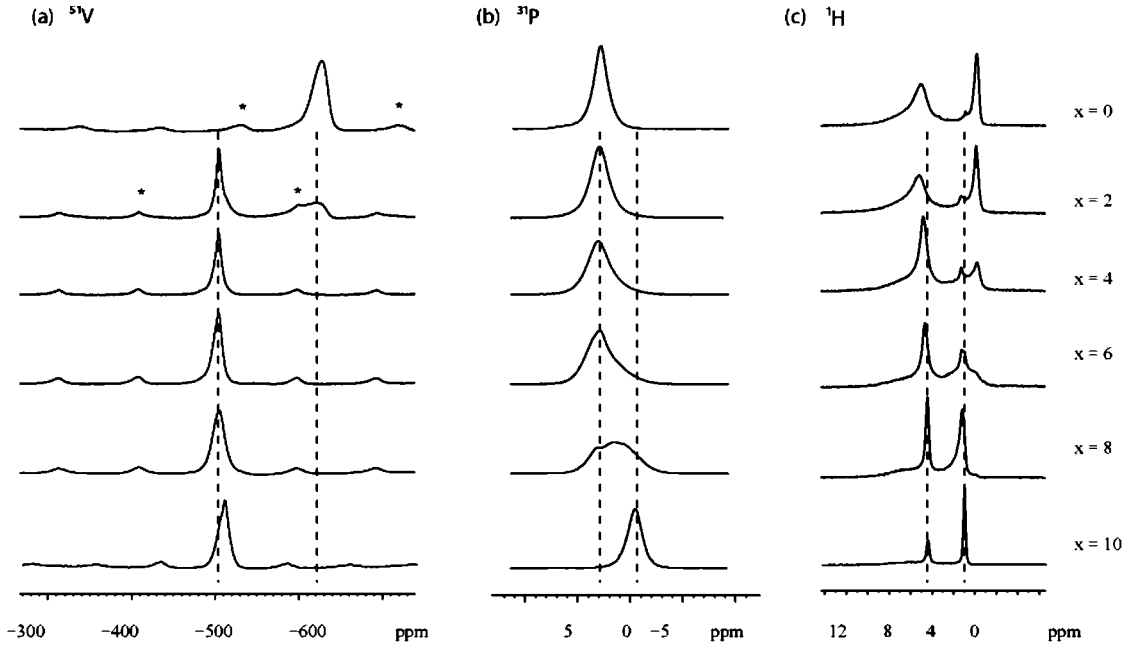

Figure 3. MAS NMR spectra of the X series $Pb_xCa_{10-x}(VO_4)(PO_4)_5(OH)_2$: (a) ^{51}V, (b) ^{31}P both one pulse and (c) ^{1}H echo NMR. The MAS rates were 10 kHz (a,b) and 25 kHz (c). The first pair of spinning sidebands in (a) is indicated by asterisks.

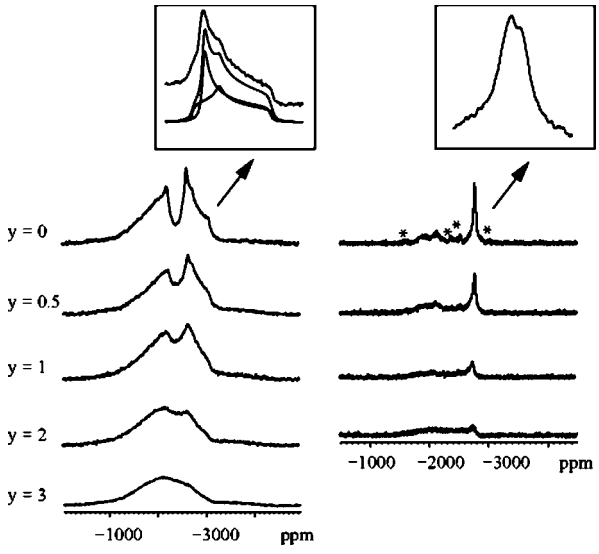

Figure 4. ^{207}Pb NMR spectra of $Pb_{10}(VO_4)_y(PO_4)_{6-y}(OH)_2$, recorded at 9.4 T. (Left) Static spin echo spectrum, the echo delay was 40 μs. (Inset: Simulation of the low-frequency signal, see text). (Right) Synchronized Echo MAS spectrum at a spin rate of 20 kHz; the echo delay was 50 μs. (Inset: Detail of the low-frequency signal). Asterisks indicate spinning sidebands.

and $x = 10$, the line width of the H_2O resonance decreases from 670 to 110 Hz and that of the hydroxyl peak from 200 to 100 Hz.

2. Vanadate Substitution of Lead Hydroxyapatite: $Pb_{10}(VO_4)_y(PO_4)_{6-y}(OH)_2$ (Y Series). Complementary information concerning structural modifications occurring in apatite solid solutions can be obtained by following the substitution of vanadates for phosphates into lead hydroxyapatites. The ^{207}Pb NMR spectra of $Pb_{10}(VO_4)_y(PO_4)_{6-y}(OH)_2$ are shown in Figure 4. The static spectrum of the pure Pb hydroxyapatite ($x = 0$) exhibits two large signals at the same position as those described in the case of the $Pb_xCa_{10-x}(VO_4)(PO_4)_5(OH)_2$ series, but with a better resolution. The relative intensity of the signals gives approximately a 3:2 ratio. The high-frequency signal has a larger chemical shift anisotropy ($\Delta\delta > 600$ ppm) than the other one ($\Delta\delta \approx 300$ ppm), which implies a lower symmetry around the Pb. The low-frequency Pb signal exhibits a well-defined but atypical CSA static line shape, while the high-frequency one has less resolved features, not showing apparent discontinuities typical of powder patterns. Neither of the signals changes with application of ^{1}H decoupling during acquisition. ^{207}Pb MAS rotation synchronized Hahn echo spectra are shown in Figure 4 (right panel). For $y = 0$, the isotropic line of the narrow low-frequency signal is clearly split into two peaks. The corresponding shifts, measured at 10 kHz spinning rate are at -2775 and -2788 ppm. It is noteworthy that these two ^{207}Pb signals show a very limited spinning rate (and thus temperature) dependence. The high-frequency ^{207}Pb resonance, on the other hand, has a larger estimated chemical shift anisotropy, and its static signal splits up under MAS into broad, low-intensity spinning sidebands, thus hampering an accurate determination of the isotropic chemical shift. Interestingly, such differing Pb sites have also been evidenced by ^{207}Pb NMR for other lead phosphates.[22,23] Attempts were made at simulating the low-frequency component of the static ^{207}Pb spectrum with two signals (Figure 4, left inset), resulting in two lines with similar chemical shift anisotropies ($\sim$300 ppm) and isotropic chemical shifts (~ -2776 and -2793 ppm), but distinct asymmetry parameters, η_σ, of $\sim$0.1 and 0.6 (Supporting Information, Table S3). The values found for the isotropic shifts are in good agreement with the MAS spectra.

As vanadate ions substitute for phosphates in the structure, both ^{207}Pb static and MAS spectra are strongly affected, with a significant loss of resolution and sensitivity. This loss of resolution of the static spectra may result from an increase in structural disorder, given the strong sensitivity of the ^{207}Pb chemical shift and CSA to the local environment. In parallel, the isotropic signals observed on the MAS spectra broaden beyond detection for $y > 2$.

In contrast with the observations made when lead enters the HA lattice (*vide supra*), the ^{1}H, ^{31}P and ^{51}V resonances do not shift much when the vanadate content is increased (Figure 5).

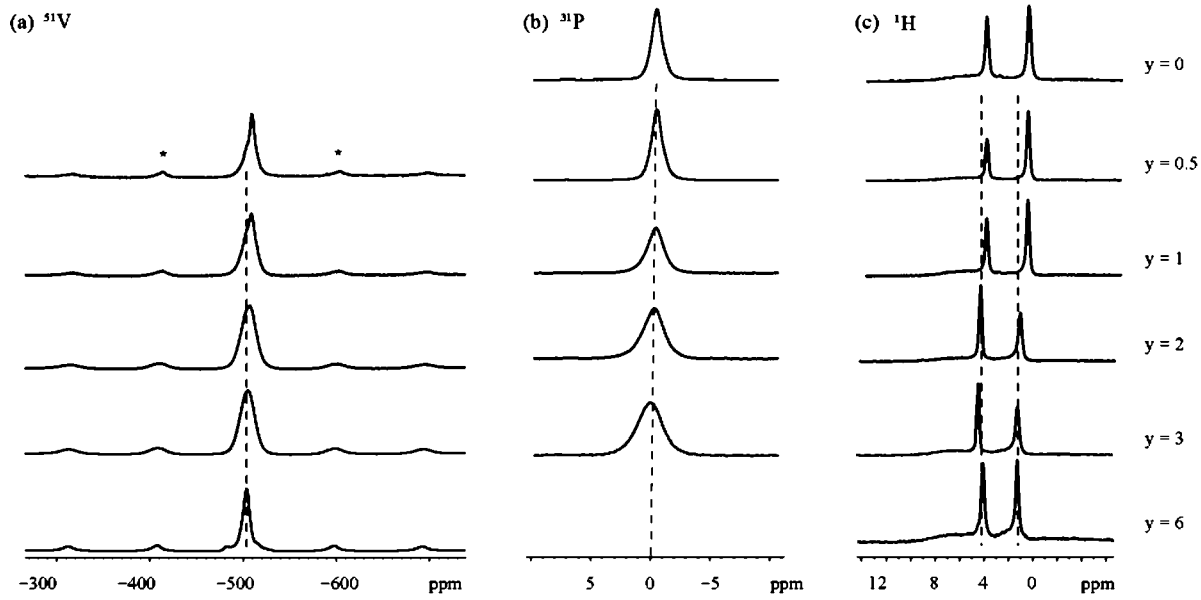

Figure 5. MAS NMR spectra of the Y series $Pb_{10}(VO_4)_y(PO_4)_{6-y}(OH)_2$: (a) ^{51}V, (b) ^{31}P both one pulse and (c) ^{1}H echo NMR. The MAS rates were 10 kHz (a,b) and 25 kHz (c). The asterisks in (a) indicate the first pair of spinning sidebands.

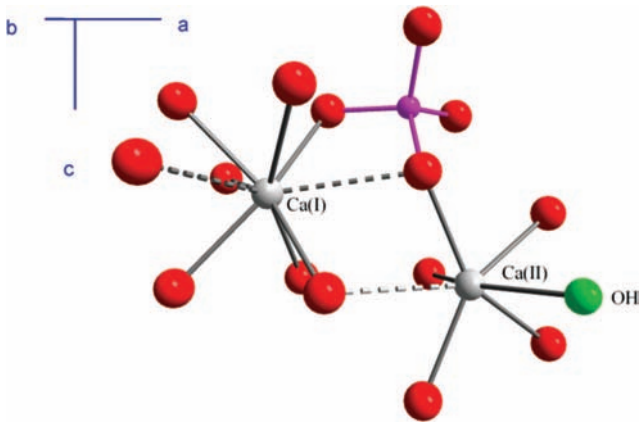

Figure 6. Representation of the cationic environment in Ca hydroxyapatite. P (or V), O, and Ca atoms are respectively in pink, red, and gray. The OH group is in green.

^{51}V MAS spectra reveal the presence of several vanadate environments, as particularly visible for low vanadium contents ($y = 0.5$, 1; see Figure 5a, and Supporting Information, Figures S4 and S5). On the other hand, when all phosphate has been substituted ($y = 6$), a single, main narrow signal is observed for ^{51}V. For the ^{31}P spectra, a moderate broadening and a minor shift of the single line is observed along the series (Figure 5b). In ^{1}H NMR, the signals of the hydroxyl group and of adsorbed water shift from 1.1 and 4.5 ppm for $y = 0$ to 1.3 and 4.1 ppm, respectively, for $y = 6$ (Figure 5c).

Discussion

Lead Substitution Sites. The structure of hydroxyapatite contains two distinct cationic sites: site (II) has a seven-fold highly distorted coordination sphere, while site (I) is located in a symmetric nine-fold coordination environment (Figure 6). The ratio between the two crystallographic M(II) and M(I) sites is 3:2. In the ^{207}Pb NMR spectra of the X and Y series of lead−vanadium hydroxyapatites (Figures 1 and 4), both Pb(I) and Pb(II) signals are well resolved. A first assignment of these signals can be obtained on the basis of their relative intensity in the static solid-echo spectrum of $Pb_{10}(PO_4)_6(OH)_2$, which has the most resolved features (in agreement with the previous observation that pure Pb hydroxyapatite has a higher symmetry than the Pb/Ca mixed preparations).[12] Indeed, for this spectrum, an integral ratio of ~3:2 is found between the peaks centered at ~−2000 and −2800 ppm, meaning that they correspond respectively to the Pb(II) and Pb(I) sites.

Using static and MAS ^{207}Pb NMR spectra, Fayon et al.[27] measured the chemical shift parameters of lead sites in a series of lead oxides, and showed that for ionic Pb^{2+} species, the isotropic chemical shifts correlate with the coordination number and mean bond length. To be more specific, the isotropic chemical shift increases directly with the coordination number and inversely with the mean Pb−O bond distance. For the apatite compounds studied here, the large negative range of chemical shifts and the line width of both signals show that Pb is in an ionic environment.[27] From the comparison of the average Pb−O bond lengths around the two sites in crystalline $Pb_{10}(PO_4)_6(OH)_2$, it appears that the Pb−O distances are shorter around the Pb(II) site,[26] meaning that its isotropic chemical shift should be at higher frequencies. Additionally, the larger CSA of the high-frequency signal and its broader MAS signals suggest an environment for this Pb site with a more anisotropic and disordered oxygen distribution, respectively. Because of the difference in local symmetry of the (I) and (II) sites, we can thus confirm the assignment of the high-frequency signal to Pb(II) and of the low-frequency one to Pb(I).

The introduction of lead into the hydroxyapatite structures has been the subject of several studies, as in this form the metal becomes unavailable biologically for a large range of pH values. In many Pb−Ca hydroxyapatite solid solutions, the Ca(II) site has been shown to be more open to cationic exchanges.[9,10,12,28,29] As shown in Figure 1, this stays the case even when vanadates are also partially substituting for phosphates in the apatite lattice.

(27) Fayon, F.; Farnan, I.; Bessada, C.; Coutures, J.; Massiot, D.; Coutures, J. P. *J. Am. Chem. Soc.* **1997**, *119*, 5212–5218.
(28) Bigi, A.; Ripamonti, A.; Brückner, S.; Gazzano, M.; Roveri, N.; Thomas, S. A. *Acta Crystallogr., Sect. B* **1989**, *B45*, 247–251.
(29) Kim, J. Y.; Hunter, B. H.; Fenton, R. H.; Kennedy, B. J. *Aust. J. Chem.* **1997**, *50*, 1061–1065.

Interestingly, Figure 1 also shows that Ca(I) occupation by lead already starts at low metal concentration ($x = 4$), in contrast to earlier reports where occupation of this site begins at lead concentrations higher than 50%.[9] In the ^{43}Ca MAS NMR spectra (Figure 2), there is a progressive decrease of the intensity of the Ca(II) signal as the lead content increases, in agreement with the fact that Pb preferentially enters this site. The ^{43}Ca NMR MAS spectrum of $Ca_{10}(VO_4)(PO_4)_5(OH)_2$ is very similar to the one previously obtained for $Ca_{10}(PO_4)_6(OH)_2$ at 18.8 T,[20] the peak positions corresponding to the two sites being nearly identical for the two compounds. However, it is noteworthy that the signals for $Ca_{10}(VO_4)(PO_4)_5(OH)_2$ are slightly broader, which could be due to a disorder-related distribution in chemical shift induced by the presence of the vanadate anions. Attempts to simulate the ^{43}Ca NMR spectra of $Pb_xCa_{10-x}(VO_4)(PO_4)_5(OH)_2$ ($x = 0, 2, 4$) showed that the lineshapes cannot be reproduced satisfactorily by using the quadrupolar parameters (C_Q and η_Q) previously found for the two calcium sites of $Ca_{10}(PO_4)_6(OH)_2$,[19] and simply varying the relative intensity of the two signals. This suggests that because of the presence of both lead and vanadate ions in the structure, the δ_{iso}, C_Q and η_Q parameters are slightly different and/or more distributed. The comparison of the ^{43}Ca spectra also suggests that the ^{43}Ca chemical shift of each site has not significantly changed after incorporation of lead. This tends to show that the average Ca−O bond distance is not strongly affected by lead substitution. In fact, previous ^{43}Ca solid-state NMR studies have shown that for compounds in which Ca is surrounded by oxygen atoms, the isotropic chemical shift decreases as the average Ca−O distance increases.[30−32] Thus, it appears that, despite the global expansion of the HA lattice caused by the incorporation of lead, calcium cations tend to maintain a given Ca−O environment within the HA structure, a piece of data not easily accessible through other spectroscopic techniques.

Structural Changes Due to Lead and Vanadium Introduction. An interesting issue in HA compounds is the position of the hydroxyls. Indeed, while remaining on average parallel to the *c*-axis, they can be either stacked in a regular head-to-tail arrangement within the columns and display a well-defined orientation from one column to the other, or they can be in a less organized arrangement within and between these columns.[7] Ordered columns alternating the OH orientation are characteristic of the monoclinic $P2_1/b$ symmetry. However, a disorder in the OH orientation is the most commonly found in HA structures, with a randomization of the OH arrangement within the columns: this corresponds to the hexagonal phase of $P6_3/m$ symmetry.[7] HA structures with either ordered or disordered hydroxyl columns have been shown to be very close in energy,[33,34] and the occurrence of the monoclinic or hexagonal phase has been shown to depend on the synthetic procedure and on the purity of the compound.[7] In the case of Pb-HA, most studies have focused on the hexagonal phase, although there is one report on a transition from a monoclinic to a hexagonal phase in the region of 400−500 K.[35] In the current case, the highest-resolution ^{207}Pb MAS NMR spectrum is obtained for $Pb_{10}(PO_4)_6(OH)_2$, where the Pb(I) resonance in the rotor-synchronized echo MAS signal splits into two lines, separated by about 10 ppm (Figure 4). The presence of two signals for this site is also suggested by simulations of the static echo spectra. In addition, the difference in the static line shape (the asymmetry parameter, Figure 4) between the two sites suggests that the two types of Pb(I) atoms are surrounded by oxygens with two different geometrical distributions. At first sight, the splitting of the Pb(I) signal seems to be incompatible with the crystallographic $P6_3/m$ hexagonal symmetry,[6] because its mirror symmetry plane implies the equivalence of all Pb(I) atoms in the unit cell. However, this symmetry element arises from the absence of *global* ordering of the position and orientation of the OH groups as an ensemble, a matter which is still widely discussed.[7] *Locally*, in the hexagonal phase, this mirror symmetry plane does not exist, as the OH groups adopt a given orientation, and small domains of aligned hydroxyls may tend to form.[12] NMR, which is sensitive to local properties, could thus be able to distinguish two different Pb(I) environments even if the Pb-HA had a crystallographic hexagonal symmetry.

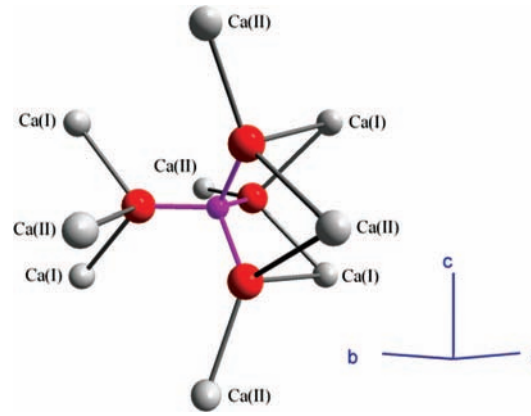

Figure 7. Anionic environment in calcium hydroxyapatite. P (or V), O and Ca atoms are respectively in pink, red and gray.

The introduction of vanadium into Pb–HA, even at the lowest content, decreases the resolution in the ^{207}Pb NMR spectra (Figure 4), a fact that can be due to the expected structural disorder. Consequently, it becomes impossible to assess if the Pb(I) sites are still distinguishable upon introduction of vanadium. Nevertheless, the two Pb peaks corresponding globally to the sites (I) and (II) remain well separated and unshifted in the spectra of the Y series for all y values.

A complementary view of the structural changes along the X and Y series comes from the spectra of the anions. The structural environment of a phosphate or vanadate anion in hexagonal hydroxyapatite is represented in Figure 7, showing that each V or P atom is surrounded by cations belonging to (I) and (II) sites in its second coordination sphere. Admitting that lead insertion at lower contents occurs exclusively at the Ca(II) site, one-third of these sites should be filled for $x = 2$. Statistically then, in the $x = 2$ sample, each P or V atom in the unit cell already possesses at least one Pb(II) in its second coordination sphere. The strong change observed in the ^{51}V NMR spectrum upon introduction of Pb (Figure 3a, $x = 0$ vs $x = 2$) suggests that V atoms are very sensitive to the presence of Pb at the Ca(II) site. In principle, this can be due to the direct influence of the neighboring heavier Pb^{2+} cation or could be caused by a major variation in the electronic density around the vanadium, such as the change in hydrogen bonding involving

(30) Dupree, R.; Howes, A. P.; Kohn, S. C. *Chem. Phys. Lett.* **1997**, *276*, 399–404.
(31) Lin, Z. J.; Smith, M. E.; Sowrey, F. E.; Newport, R. J. *Phys. Rev. B: Condens. Mater. Phys.* **2004**, *69*, 224107.
(32) Wong, A.; Howes, A. P.; Dupree, R.; Smith, M. E. *Chem. Phys. Lett.* **2006**, *427*, 201–205.
(33) Calderin, L. *Phys. Rev. B: Condens. Mater. Phys.* **2003**, *67*, 134106.
(34) Rulis, P. *Phys. Rev. B: Condens. Mater. Phys.* **2004**, *70*, 155104.
(35) Hadrich, A.; Lautié, A.; Mhiri, T. *J. Raman Spectrosc.* **2001**, *32*, 33–40.

vanadate oxygen atoms, although any definitive interpretation of the isotropic chemical shift in terms of protonation states is difficult in the case of ^{51}V.[36] Concerning the latter point, because vanadates in HA structures are known to engage in strong hydrogen bonds,[37] and given that the introduction of Pb induces an increase of the unit cell volume, it is possible that some of the pre-existing hydrogen bonds do not survive such an expansion. However, further investigation would be required to reveal the actual mechanism responsible for the ^{51}V NMR spectral variation (especially between $x = 0$ and $x = 2$), all the more since the isotropic chemical shift of ^{51}V in solid-state NMR spectra are rarely used as a definitive indicator of specific structural changes.[24] In any case, such a dramatic change in the ^{51}V spectrum upon lead insertion correlates well with the completely different redox[5,6] behavior observed for $Ca_{10}(VO_4)_y(PO_4)_{6-y}(OH)_2$ and $Pb_{10}(VO_4)_y(PO_4)_{6-y}(OH)_2$. The changes in the V surroundings observed by NMR may indicate an increase in availability of the redox sites due to Pb exchange.

The ^{31}P MAS NMR spectra of the two extreme members for the X series ($x = 0$ and $x = 10$) both show one relatively narrow line, but at different positions (~0 ppm for $x = 10$, vs ~3.3 ppm for $x = 0$). Most interestingly, the evolution of the ^{31}P signal along the X series reveals the presence of several intermediate species, as shown by the overlapping signals in Figure 3b. This effect is particularly noteworthy starting at $x = 6$, a composition which has been shown to correspond to specific changes in the c parameter and to a deviation from Vegard's law (see Supporting Information, Figure S2).[38] Conversely, along the Y series, ^{31}P MAS NMR spectra do not exhibit large variations (Figure 5b) with the exception of an increase in line width as the vanadium content rises. Thus, the introduction of vanadates does not seem to significantly affect the local geometry around the phosphate unit in the modified HA structure.

Several reasons could be invoked to explain the shift of the ^{31}P signal in the X series. Indeed, numerous studies have shown that ^{31}P shielding in phosphate compounds increases with increasing π-bond order between phosphorus and oxygen (leading to shorter P−O bonds).[39−43] The formation of hydrogen bonds can also produce variations in the ^{31}P chemical shift of the order observed here.[44] The broadening of the phosphorus signals along this series, especially for $x = 6$ and 8 mirrors well the known onset of structural disorder associated with these specific solid solutions.[10] Interestingly, this is not directly paralleled in the corresponding ^{51}V NMR spectra, where the signal progressively broadens along the X series and several contributions become noticeable for $x = 10$ (see Supporting Information, Figure S5), as a further confirmation of the relative insensitivity of vanadium chemical shifts to the local environment.

An analysis of the ^{51}V spectra of the Y series reveals the presence of several inequivalent vanadium sites for $y = 0.5$ and 1 (Figure 5a and Supporting Information, Figures S4 and S5), which progressively merge into a single line for $y \geq 2$. However, the narrow range of this chemical shift distribution testifies that the nature of the neighboring anions (phosphate or vanadate) has a direct but small influence on vanadium's electronic environment.

Because the hydroxyls and, in general, the hydrogen-bonding network can be involved in the structural changes of HA and in its acid properties, it is particularly interesting to examine the proton NMR spectra of these phases.

Along the X series (Figure 3c), the two main OH peaks corresponding to the extreme Pb loading levels (at −0.2 ppm for $x = 0$ and at ~1.1 ppm for $x = 10$) can be assigned to "Ca−OH" and "Pb−OH" units respectively, as their relative intensity varies as the lead concentration increases. Intermediate compositions corresponds to more complex spectra, in perfect analogy with the ^{31}P NMR, providing further evidence of a structural discontinuity and a distribution of environments at this particular composition. The deshielding of the hydroxyl proton to 1.1 ppm in pure Pb hydroxyapatite could be due to the lengthening of the O−H bond, as a result of the interaction of the OH with the more electronegative lead cation, and of the more covalent character of the Pb−O bonds compared to Ca−O bonds.[45−47] On the other hand, an effect due to changes in hydrogen bonding cannot be ruled out.

Another notable feature is the evolution of the proton signal line width. The high spinning rate ^1H MAS NMR spectrum of $Ca_{10}(VO_4)(PO_4)_5(OH)_2$ ($x = 0$) is very similar to the one described for $Ca_{10}(PO_4)_6(OH)_2$,[48] with broad signals at ~5 and 0 ppm for water and hydroxyls, respectively. Conversely, the strong narrowing of the proton peaks for the $x = 10$ phase suggests that OH groups as well as water molecules become more mobile when Pb^{2+} is inserted instead of Ca^{2+}. The description of the overall proton mobility in solids is a complex issue, involving spatial reorientation, chemical exchange and site hopping.[49] In our case the changes in the line shape accompany closely the increase of the c parameter, and hence the lattice volume, observed with the changes in the Pb content.

Conclusions

The simultaneous uptake of vanadium and lead in various relative concentrations into hydroxyapatite structures has been followed by solid-state NMR on two series of model compounds: $Pb_xCa_{10-x}(VO_4)(PO_4)_5(OH)_2$ ($x = 0-10$) and $Pb_{10}(VO_4)_y(PO_4)_{6-y}(OH)_2$ ($y = 0-6$). The preferential incorporation of lead into the Ca(II) site has been confirmed by examination of the ^{207}Pb and ^{43}Ca NMR spectra. The occupation of site (I) by lead cations is found to start at ~40% substitution level. The cosubstitution of vanadium and lead produces less ordered materials. The coexistence of intermediate environments observed for mixed Pb/Ca hydroxyapatites is particularly note-

(36) Waller, M.; Bühl, M.; Geethalakshmi, K.; Wang, D.; Thiel, W. *Chem. -Eur. J.* **2007**, *13*, 4723–4732.
(37) Higesrolando, F. J.; Andresverges, M.; Gonzalezdiaz, P. F. *Spectrochim. Acta, Part A* **1982**, *38*, 197–203.
(38) Kaflak-Hachulska, A.; Samoson, A.; Kolodziejski, W. *Calcif. Tissue Int.* **2003**, *73*, 476–486.
(39) Letcher, J. H.; Van Wazer, J. R. *J. Chem. Phys.* **1966**, *44*, 815–829.
(40) Costello, A. J. R.; Glonek, T.; Van Wazer, J. R. *Inorg. Chem.* **1976**, *15*, 972–974.
(41) Un, S.; Klein, M. P. *J. Am. Chem. Soc.* **1989**, *111*, 5119–5124.
(42) Cheetham, A. K.; Clayden, N. J.; Dobson, C. M.; Jakeman, R. J. B. *J. Chem. Soc., Chem. Commun.* **1986**, 195–197.
(43) Aime, S.; Digilio, G.; Gobetto, R.; Bigi, A.; Ripamonti, A.; Roveri, N.; Gazzano, M. *Inorg. Chem.* **1996**, *35*, 149–154.
(44) Caldarelli, S.; Meden, A.; Tuel, A. *J. Phys. Chem. B* **1999**, *103*, 5477–5487.
(45) Mathew, M.; Brown, W. E.; Austin, M.; Negas, T. *J. Solid State Chem.* **1980**, *35*, 69–76.
(46) Sugiyama, S.; Nakanishi, T.; Ishimura, T.; Moriga, T.; Hayashi, H.; Shigemoto, N.; Moffat, J. B. *J. Solid State Chem.* **1999**, *143*, 296–302.
(47) Sugiyama, S.; Moriga, T.; Hayashi, H.; Moffat, J. B. *Bull. Chem. Soc. Jpn.* **2001**, *74*, 187–192.
(48) Yesinowski, J. P.; Eckert, H. *J. Am. Chem. Soc.* **1987**, *109*, 6274–6282.
(49) Kanellopoulos, J.; Gottert, C.; Schneider, D.; Knorr, B.; Prager, D.; Ernst, H.; Freude, D. *J. Catal.* **2008**, *255*, 68–78.

worthy at lead loadings of ~60%, as seen by the ^{31}P and ^{1}H NMR spectra. The ^{51}V and ^{31}P spectra of $Pb_xCa_{10-x}(VO_4)(PO_4)_5(OH)_2$ compounds show that Pb introduction seems to affect more the vanadium environment than the phosphorus one, which suggests slight differences in the local structure of these two anions. This could be one of the reasons for the enhanced redox and catalytic activity previously observed upon introduction of lead into vanadium hydroxyapatite. On the contrary, for the $Pb_{10}(VO_4)_y(PO_4)_{6-y}(OH)_2$ series, vanadium incorporation has no strong effect on the NMR spectra, other than introducing a generalized line broadening, associated with the increase in structural disorder. Thus, the lead−hydroxyapatite structure seems rather insensitive to the introduction of vanadates. Finally, in the case of $Pb_{10}(PO_4)_6(OH)_2$, two Pb(I) sites have been resolved, which could be consistent with the crystallographic hexagonal $P6_3/m$ symmetry of the apatite, because locally the symmetry is reduced.

Although the variety of existing modified hydroxyapatite structures extends well beyond the scope of the present work, our study here shows that the local environment of all the ions which constitute these species is worth investigating by NMR, as it brings out very valuable structural information, which is likely to shed light on the functional properties of these materials. Similar studies should thus be carried out when trying to design or understand the properties of substituted apatites, including those of natural compounds like bone and its substitutes.

Acknowledgment. This work was partly supported by CAPES-COFECUB Grant Number 436/03 and by the ARCUS program of the MAEE and the Region PACA. J.-G.E. and A.M.R. thank CNPq (Conselho Nacional de Desenvolvimento e Pesquisa) of Brazil for support. D.L. thanks the 6th European Community Framework Program for a Marie Curie IEF and Dr. Alan Wong for his help in the ^{43}Ca NMR experiments. EPSRC and the University of Warwick are thanked for partial funding of the NMR work at Warwick.

Supporting Information Available: ^{51}V Static Echo NMR spectrum of $Ca_{10}(VO_4)(PO_4)_5(OH)_2$. Results of fit of the 10 kHz ^{207}Pb MAS spectrum of $Pb_{10}(PO_4)_6(OH)_2$, and of a deconvolution of: the ^{31}P MAS spectrum of $Pb_6Ca_4(PO_4)_5(VO_4)(OH)_2$, the ^{51}V MAS spectrum of $Pb_{10}(VO_4)_{0.5}(PO_4)_{5.5}(VO_4)_{0.5}(OH)_2$ and of the ^{51}V MAS spectrum of $Pb_{10}(VO_4)(PO_4)_5(OH)_2$. This material is available free of charge via the Internet at http://pubs.acs.org.

JA808270V